



**Cite this article:** Suda N, Sunayama H, Kitayama Y, Kamon Y, Takeuchi T. 2017

Oriented, molecularly imprinted cavities with dual binding sites for highly sensitive and selective recognition of cortisol. *R. Soc. open sci.* **4**: 170300.

<http://dx.doi.org/10.1098/rsos.170300>

Received: 4 April 2017

Accepted: 17 July 2017

**Subject Category:**

Chemistry

**Subject Areas:**

analytical chemistry/biomimetics

**Keywords:**

molecular imprinting, stress marker, cortisol, molecular recognition, competitive binding assay, saliva

**Author for correspondence:**

Toshifumi Takeuchi

e-mail: [takeuchi@gold.kobe-u.ac.jp](mailto:takeuchi@gold.kobe-u.ac.jp)

This article has been edited by the Royal Society of Chemistry, including the commissioning, peer review process and editorial aspects up to the point of acceptance.

Electronic supplementary material is available online at <https://dx.doi.org/10.6084/m9.figshare.c.3843643>.

# Oriented, molecularly imprinted cavities with dual binding sites for highly sensitive and selective recognition of cortisol

Narito Suda, Hirobumi Sunayama, Yukiya Kitayama, Yuri Kamon and Toshifumi Takeuchi

Graduate School of Engineering, Kobe University, 1-1 Rokkodai-cho, Nada-ku, Kobe 657-8501, Japan

TT, 0000-0002-5641-2333

Novel, molecularly imprinted polymers (MIPs) were developed for the highly sensitive and selective recognition of the stress marker cortisol. Oriented, homogeneous cavities with two binding sites for cortisol were fabricated by surface-initiated atom transfer radical polymerization, using a cortisol motif template molecule (TM1) which consists of a polymerizable moiety attached at the 3-carbonyl group of cortisol via an oxime linkage and an adamantane carboxylate moiety coupled with the 21-hydroxyl group. TM1 was orientationally immobilized on a  $\beta$ -cyclodextrin ( $\beta$ -CD)-grafted gold-coated sensor chip by inclusion of the adamantane moiety of TM1, followed by copolymerization of a hydrophilic comonomer, 2-methacryloyloxyethyl phosphorylcholine, with or without a cross-linker, *N,N'*-methylenebisacrylamide. Subsequent cleavage of the oxime linkage leaves the imprinted cavities that contain dual binding sites—namely, the aminoxy group and  $\beta$ -CD—capable of oxime formation and hydrophobic interaction, respectively. As an application, MIP-based picomolar level detection of cortisol was demonstrated by a competitive binding assay using a fluorescent competitor. Cross-linking of the MIP imparts rigidity to the binding cavities, and improves the selectivity and sensitivity significantly, reducing the limit of detection to 4.8 pM. In addition, detection of cortisol in saliva samples was demonstrated as a feasibility study.

## 1. Introduction

Cortisol is a stress biomarker secreted from the adrenal gland in response to stress. Thus, the highly sensitive detection of cortisol



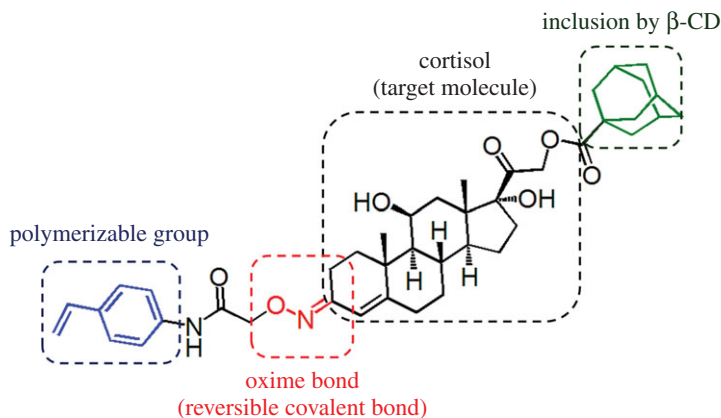


**Figure 1.** The TM1 template molecule, designed for cortisol imprinting.

has been used to diagnose mental disorders. Representative methods of detecting cortisol include enzyme-linked immunosorbent assay and mass spectrometry [1–4]. However, widespread use of these methods in self-medication and general healthcare facilities is limited by the high costs of unstable natural proteins, expensive instruments and complicated procedures.

Molecularly imprinted polymers (MIPs), known as polymer-based artificial receptors, have attracted significant attention because of their high stability, low cost and capabilities gained by further functionalization such as stimuli-responsiveness and signal transduction [5–13]. Typically, MIPs are synthesized by radical copolymerization of template molecules covalently or non-covalently conjugated with functional monomers, comonomers and cross-linking agents. The subsequent removal of the template molecules from the resulting polymers yields MIPs with specific binding cavities for the template molecules, which are complementary in size and shape.

Several cortisol-imprinted polymers have been previously reported [14,15]. They were typically prepared using a single functional monomer because plural binding sites in an imprinted cavity appeared to indicate more sensitive and selective binding activity towards target molecules such as nucleobases [16,17], endocrine desolators [18], herbicides [19], antibiotics [20,21], proteins [22–26], glycans [27–29], organic pollutants [30,31] and enzyme inhibitors [32,33]. We have reported cortisol-MIPs prepared with the ability to recognize cortisol using cortisol-21-monomethacrylate and itaconic acid as the template molecule and functional monomer, respectively. Moreover, a cortisol nanosensor platform based on the MIP particles and fluorescent-labelled cortisol was successfully demonstrated [34,35]. However, the limit of detection (*ca* 80 nM) was not sufficient for practical use.

Recently, an approach for the precise formation of oriented protein recognition cavities in MIP thin layers, with high affinity and selectivity towards the target protein, was developed using immobilized template protein molecules via well-defined protein–ligand interactions. The specific ligand served both as the protein-immobilizing agent during the surface-initiated controlled/living radical polymerization, and as the interaction site for the target protein after the construction of the imprinted binding cavity [36]. To date, this strategy can be applied only to proteins with binding sites for specific ligands, and further extension to other targets such as small molecules is still a challenging task. Thus, MIPs are highly specific and sensitive molecular recognition materials that can provide an alternative to natural antibodies for small molecules, which are not easily available.

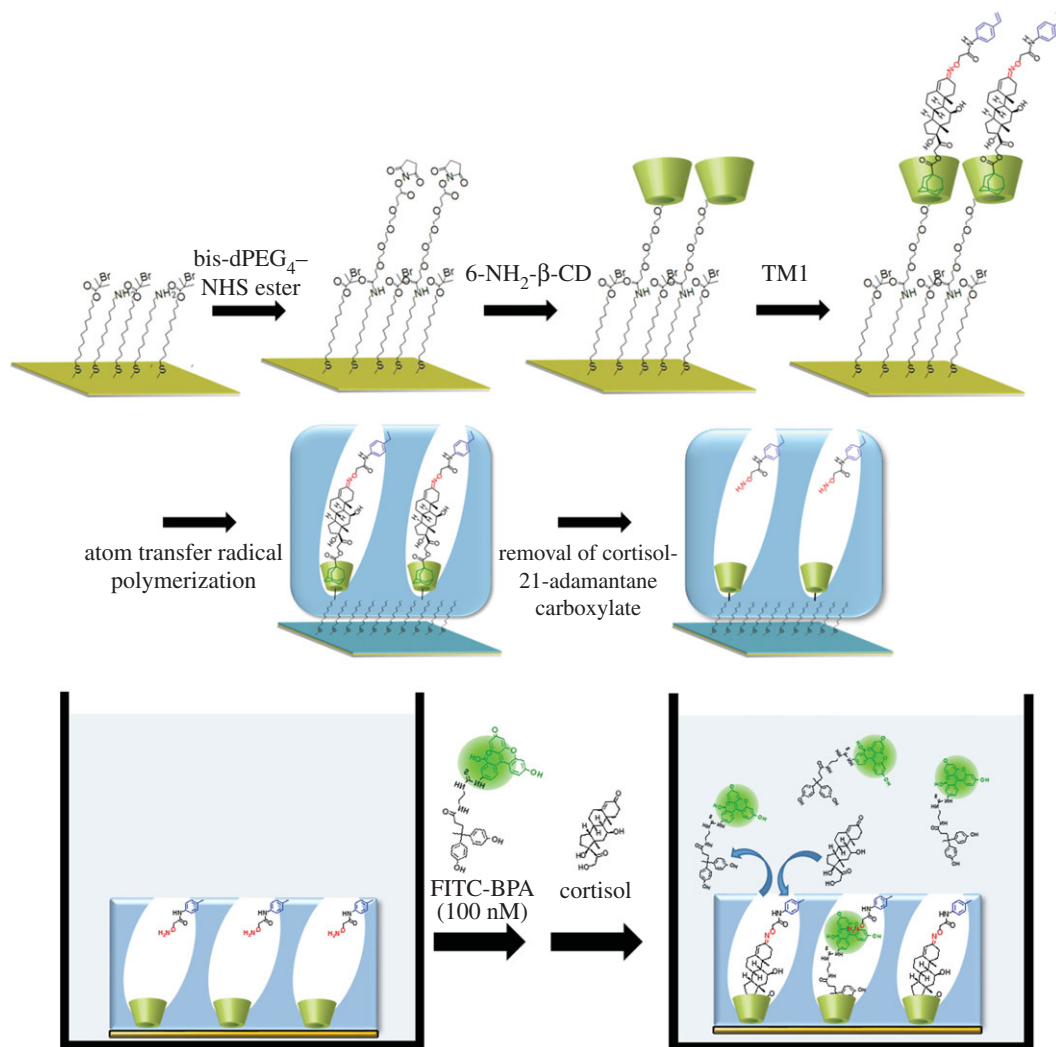
In this study, a novel cortisol motif template molecule (TM1), cortisol-3-oxime- $\{O$ -[ $N$ -(4-vinylphenyl)]acetamide $\}$ -21-adamantane carboxylate (figure 1), was designed to construct MIP thin layers with orientated binding cavities that contained two interaction sites for cortisol. TM1 is composed of a cortisol molecule linked to 2-aminoxy- $N$ -(4-vinylphenyl)acetamide at the 3-carbonyl group through reversible oxime bond formation [37–40] and to 1-adamantane carboxylic acid at the 21-hydroxyl group through ester formation. The adamantane moiety can interact with  $\beta$ -cyclodextrin ( $\beta$ -CD) by hydrophobic inclusion [41–43]. The reversible oxime linkage enables the removal of TM1 from the cortisol-imprinted cavity, and the resulting aminoxy group can serve as the interaction site for the 3-carbonyl group of cortisol. The adamantyl group induces the orientational immobilization of TM1 on a  $\beta$ -CD-grafted gold-coated glass substrate by hydrophobic interaction. The polymerization is conducted using 2-methacryloyloxyethyl phosphorylcholine (MPC) as a biocompatible comonomer, and subsequent removal of TM1 by hydrolysis of the oxime bond followed by washing with ethanol

leaving the aminoxy group and the  $\beta$ -CD moiety within the imprinted cavity. Surface-initiated atom transfer radical polymerization using activators generated by electron transfer (SI-AGET ATRP) [44–50] is employed to form a homogeneous polymer matrix around the imprinted cavities, resulting in MIP thin layers with the desired thickness and low non-specific binding properties [51]. Herein, a highly sensitive cortisol detection technique was developed based on a fluorescence competitive binding assay using a fluorescent-labelled competitor in standard aqueous solutions and saliva samples. This method demonstrates that oriented, molecularly imprinted cavities with dual binding sites have significant potential as a powerful, cost-effective and rational tool to provide a synthetic alternative to natural antibodies to low molecular weight compounds.

## 2. Results and discussion

TM1 consists of cortisol-21-adamantane carboxylic acid ester, which is capable of forming inclusion complexes with  $\beta$ -CD, linked with a polymerizable aminoxy moiety at the 3-carbonyl group of cortisol through a reversible oxime bond (figure 1; electronic supplementary material, scheme S1). A mixed, self-assembled monolayer (SAM) is formed on the surface of a gold-coated glass substrate to introduce amino and bromo groups (initiators of SI-AGET ATRP) on the surface (scheme 1a). In order to orientationally immobilize TM1 on the substrate, 6-NH<sub>2</sub>- $\beta$ -CD; (electronic supplementary material, scheme S2) is coupled with the amino groups on the substrate via bis-dPEG<sub>4</sub>-NHS ester. The interaction between  $\beta$ -CD and the adamantyl group of TM1 was confirmed by <sup>1</sup>H-NMR (electronic supplementary material, figure S1), while no interaction was observed between  $\beta$ -CD and the styryl group of TM1. The subsequent immobilization of TM1 is carried out by inclusion of the TM1 adamantane moiety into the immobilized  $\beta$ -CD in aqueous solution. The oriented immobilization of TM1 can be achieved because of preferable inclusion of the 21-adamantane moiety compared with the *N*-(4-vinylphenyl)acetamide moiety. According to previous reports, such oriented immobilization enables the construction of homogeneous binding cavities, unlike conventional MIP preparation techniques [52–55]. Next, SI-AGET ATRP of MPC was conducted on the TM1-conjugated gold-coated glass substrate, with or without *N,N'*-methylenebisacrylamide (MBAAm) addition and using CuBr<sub>2</sub>/*N,N,N',N''*-pentamethyldiethylenetriamine (PMDETA) as the catalyst. The phospholipid-mimetic, biocompatible MPC monomer [56] was chosen as the comonomer to make the polymer matrix hydrophilic and to reduce non-specific binding of off-target proteins, which may interfere with cortisol recognition in real samples. After polymerization, TM1 was removed by cleaving the oxime linkage by acid hydrolysis [57]. The SAM and the MPC polymer matrix are confirmed to be stable under the acidic conditions employed (electronic supplementary material, table S1). In order to confirm formation of the MIP thin layer on the substrate via SI-AGET ATRP, elemental analysis was conducted using X-ray photoelectron spectroscopy. After polymerization, a P 2*p* peak with a maximum at around 134 eV is observed, and is attributed to the phosphorylcholine group (electronic supplementary material, figure S2), which indicates that the poly(MPC) layer was successfully formed on the gold-coated glass substrate. In addition, X-ray reflectometry measurements were performed to evaluate the thickness of the MIP thin layer (electronic supplementary material, figure S3 and table S2). After 30 min of polymerization, the thickness is estimated to be approximately 3 nm, and the polymerization proceeds linearly with time, indicating that the MIP thin layer formation takes place in a living manner (electronic supplementary material, figure S4).

The binding activity of the MIP thin layers towards cortisol is evaluated by a competitive binding assay (scheme 1b). Because bisphenol A (BPA) is known as a possible endocrine disruptor and can bind to glucocorticoid receptors [58,59], fluorescein-conjugated BPA (FITC-BPA) is prepared as a novel fluorescent competitor for cortisol binding (electronic supplementary material, scheme S3). Since a possible complex of FITC-BPA and  $\beta$ -CD (approx. 20 Å) is estimated to be the same size as TM1 and  $\beta$ -CD (electronic supplementary material, figure S5) via a molecular mechanics-based docking simulation under aqueous conditions (dielectric constant = 80), FITC-BPA is expected to be an accessible competitor for the imprinted cavity. In the competitive binding assay, FITC-BPA first interacts with the MIP, then adds cortisol, resulting in desorption of FITC-BPA from the binding cavities depending on the concentration of cortisol added. In order to confirm whether FITC-BPA functions as a competitor, i.e. has a moderate affinity for cortisol binding sites, FITC-BPA (final concentration 0–400 nM) was incubated in the presence of the MIP thin layer in a 10 mM phosphate buffer (pH 7.4). The incubation time was set to 20 min, which allows a constant fluorescence intensity value (electronic supplementary material, figure S6). The fluorescence intensity derived from unbound FITC-BPA in the supernatant was measured.



**Scheme 1.** Preparation of the cortisol-MIP thin layer containing oriented cavities with dual binding sites within the imprinted cavity (*a*) and schematic of the competitive binding assay using FITC-BPA as the fluorescent competitor (*b*).

A fluorescence intensity change ( $\Delta I = I - I_0$ ) was used as an index for identification of binding events ( $I_0$  and  $I$  are defined as the fluorescence intensities before and after the incubation of FITC-BPA with the MIP thin layer, respectively). The  $\Delta I$  values decrease with the addition of FITC-BPA, indicating that FITC-BPA is able to bind to the cortisol binding cavities in the MIP thin layer, and that the binding cavities are almost saturated with 100 nM FITC-BPA (electronic supplementary material, figure S7). It should be noted that no fluorescence change is detected upon interaction between free cortisol and free FITC-BPA. When various concentrations of cortisol are added to the buffer solution containing 100 nM FITC-BPA, no fluorescence change is observed (electronic supplementary material, figure S8), confirming that cortisol does not interact with FITC-BPA during the competitive binding assay.

In order to examine the binding behaviour of cortisol towards the MIP thin layer, fluorescence measurements of the FITC-BPA released by competitive cortisol binding were performed (figure 2*a*). The MIP was immersed in the buffer solution containing 100 nM FITC-BPA, and various amounts of cortisol (final concentration 0–0.4 nM) were added, followed by incubation for 20 min. The relative fluorescence intensity change ( $\Delta I/I_0$ ) caused by the FITC-BPA released from the MIP thin layer because of the competitive binding was measured. The incubation time was set at 20 min, because the  $\Delta I/I_0$  value remained constant 20 min after the addition of cortisol (electronic supplementary material, figure S9). The  $\Delta I/I_0$  values in the supernatant increase with the cortisol concentration, and the poly(MPC) itself (only the polymer matrix) does not respond to the competitive binding assay under the same conditions described above (electronic supplementary material, figure S10).

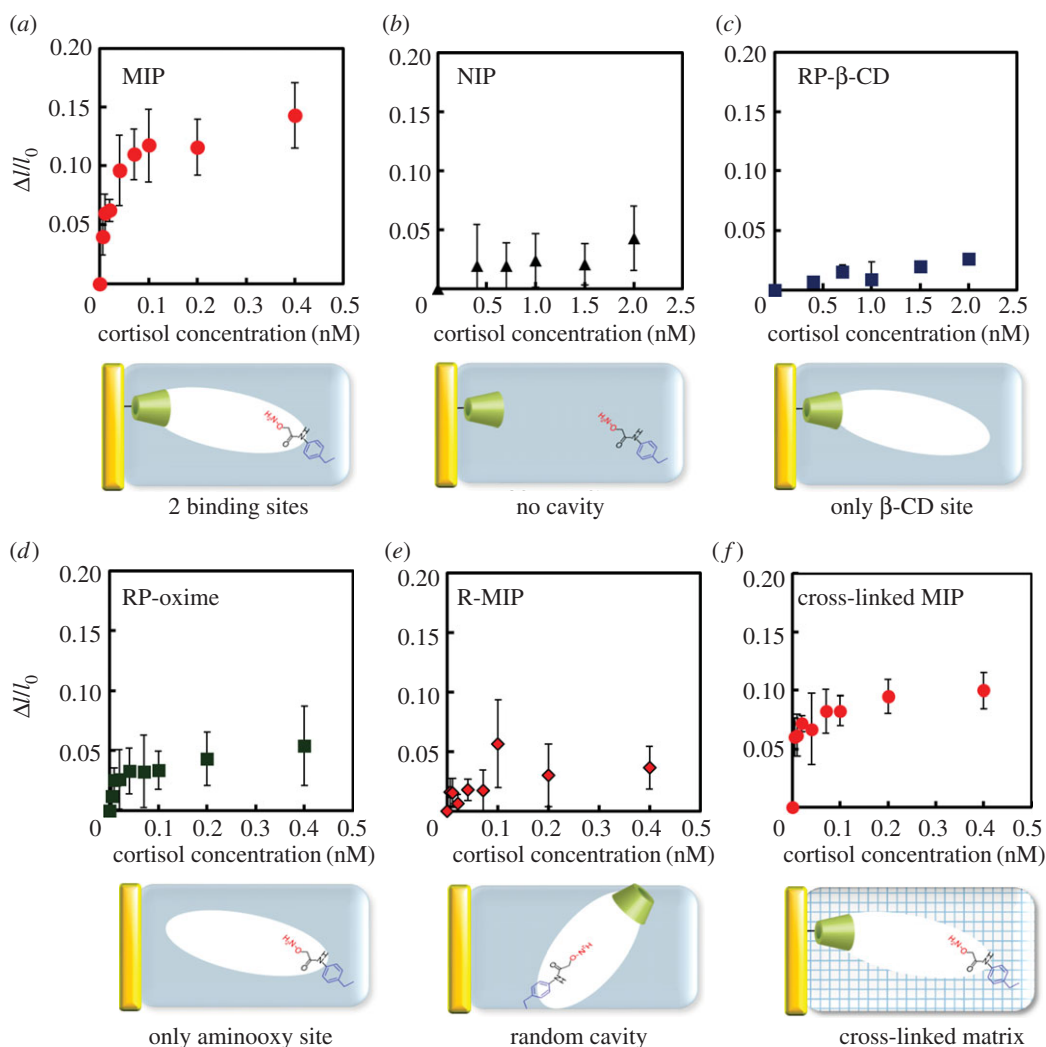


**Figure 2.** Competitive cortisol binding and FITC-BPA (100 nM) to MIP (a), NIP (b), RP- $\beta$ -CD (c), RP-oxime (d), R-MIP (e) and cross-linked MIP (f) in 10 mM phosphate buffer (pH 7.4).

The apparent binding constant ( $K_a$ ) of the non-cross-linked MIP thin layer is estimated to be  $1.28 \times 10^{11} \text{ M}^{-1}$  by curve fitting using DeltaGraph v. 5.4.5 (electronic supplementary material, figure S11a). The limit of detection is 7.1 pM, as calculated using  $3 \text{ s.d.}/m$  ( $m$ : slope of the linear part of the binding isotherm, s.d.: standard deviation) [60], which confirms that the imprinting process enables installation of the aminoxy group and the  $\beta$ -CD moiety in a position more favourable for the specific cortisol binding.

A non-imprinted polymer (NIP) with randomly located aminoxy groups and  $\beta$ -CD-immobilized on the substrate is prepared without the use of TM1 (no imprinted cavity for cortisol; electronic supplementary material, scheme S4). Binding NIP experiments are conducted and compared with the results obtained for MIP (figure 2a): the  $\Delta I/I_0$  values for NIP are very small (figure 2b) and the apparent  $K_a$  ( $3.93 \times 10^{10} \text{ M}^{-1}$ ) is 3.3 times smaller than that of MIP (electronic supplementary material, figure S11b), revealing that the TM1 imprinting process induces a high affinity and, therefore, confirming the efficiency of the imprinting effect.

In order to evaluate the effectiveness of the dual binding sites in the imprinted cavity, two reference MIP thin layers with only one binding site to either the immobilized  $\beta$ -CD (RP- $\beta$ -CD; electronic supplementary material, scheme S5) or the aminoxy group (RP-oxime; electronic supplementary material, scheme S6) in the imprinted cavity were prepared. The  $\Delta I/I_0$  values for RP- $\beta$ -CD (figure 2c) and RP-oxime (figure 2d) are also clearly smaller than those for MIP, and the apparent  $K_a$  values are 180 times ( $6.99 \times 10^8 \text{ M}^{-1}$ ; electronic supplementary material, figure S11c) and 3 times ( $4.00 \times 10^{10} \text{ M}^{-1}$ ; electronic supplementary material, figure S11d) smaller than that of MIP, respectively. Based on these results, the



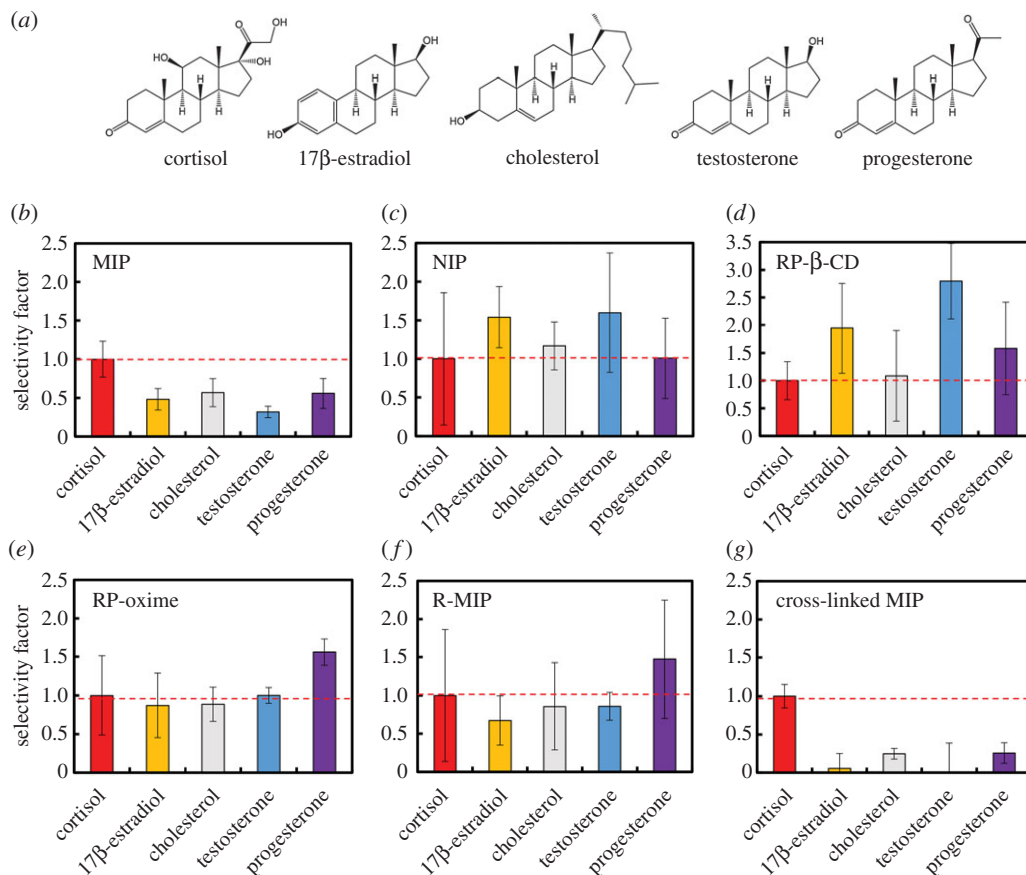


**Figure 3.** Chemical structures of cortisol and its tested structural analogues (a), and selectivities of MIP (b), NIP (c), RP- $\beta$ -CD (d), RP-oxime (e), R-MIP (f) and cross-linked MIP (g) towards cortisol, 17 $\beta$ -estradiol, cholesterol, testosterone and progesterone. The selectivity factor was obtained from the ratio of  $(\Delta I/I_0)_{\text{reference compound}}$  to  $(\Delta I/I_0)_{\text{cortisol}}$ .

dual binding sites are effective in developing a strong affinity towards cortisol. The effect of orientation of the imprinted cavities in MIP was proved by comparison with R-MIP containing randomly located cortisol-imprinted cavities with dual binding sites (electronic supplementary material, scheme S7), which was prepared using *N*-methacryloyl 6-amido- $\beta$ -CD (6-MAm- $\beta$ -CD; electronic supplementary material, scheme S2) and TM1. The  $\Delta I/I_0$  values for R-MIP (figure 2e) were again smaller than those for MIP, and the apparent  $K_a$  was found to be three times smaller than that of MIP ( $4.01 \times 10^{10} \text{ M}^{-1}$ ; electronic supplementary material, figure S11e), confirming that the orientation of the imprinted cavities can enhance the affinity of MIP towards cortisol.

Because cross-linking of the polymer matrices was reported to affect the affinity and selectivity of the resultant MIPs for proteins [61], a cross-linked MIP is prepared using MBAAM as a hydrophilic cross-linker with 20 mol% of MPC (figure 2f). The apparent  $K_a$  value of the cross-linked MIP is estimated to be  $2.30 \times 10^{11} \text{ M}^{-1}$  (electronic supplementary material, figure S11f), and the limit of detection is 4.8 pM. Thus, cross-linking during the imprinting process can enhance the affinity, which becomes comparable to that of antibodies [61,62]. The level of error appeared to decrease when the MIP was cross-linked, suggesting that reproducibility is influenced by the stability of the MIP surface, and can be improved by optimizing the cross-linker ratio and/or screening the cross-linking agents.

In order to evaluate the effect of cross-linking on selectivity, the selectivities of MIP, NIP, RP- $\beta$ -CD, RP-oxime, R-MIP and cross-linked MIP towards structural analogues of cortisol (figure 3a), such as 17 $\beta$ -estradiol (phenolic and aliphatic hydroxyl groups at C3 and C17, respectively), cholesterol (hydroxyl group at C3), testosterone (keto and hydroxyl groups at C3 and C20, respectively) and progesterone (two ketone moieties), were examined. The selectivity factor, defined as the ratio between  $(\Delta I/I_0)_{\text{reference compound}}$  and  $(\Delta I/I_0)_{\text{cortisol}}$ , was used as an index of the selective binding capability. A value of less than 1 indicates high selectivity towards cortisol.

For MIP, the selectivity factors for all reference compounds are less than 1; the values of 0.48, 0.57, 0.32 and 0.56 are for 17 $\beta$ -estradiol, cholesterol, testosterone and progesterone, respectively (figure 3b),

whereas NIP shows non-specific binding behaviour, with values of 1 or higher: 1.54, 1.17, 1.60 and 1.01 for  $17\beta$ -estradiol, cholesterol, testosterone and progesterone, respectively (figure 3c). The lower selectivity of NIP towards cortisol demonstrates the influence of the imprinting effect. RP- $\beta$ -CD shows a similar trend to that of NIP, with higher binding activity for  $17\beta$ -estradiol (1.94), testosterone (2.79) and progesterone (1.58) than cortisol (figure 3d). This may be due to hydrophobic interactions with  $\beta$ -CD and to the more flexible side chains of cortisol and cholesterol, which may interfere with inclusion. RP-oxime and R-MIP show almost no selectivity (figure 3e,f), suggesting that the aminoxy group cannot form an oxime bond without the cooperative binding of  $\beta$ -CD, as also demonstrated by the fact that  $17\beta$ -estradiol and cholesterol, which have no keto group, were bound in a similar manner as the other compounds. Thus, precise molecular recognition of cortisol is attributed to a dual point binding based on oxime formation and inclusion by  $\beta$ -CD.

Interestingly, as described above, the cross-linked MIP exhibits not only enhanced affinity but also remarkably higher selectivity towards cortisol than the other polymer matrices (figure 3g), with almost no cross-reactivity for testosterone and a  $17\beta$ -estradiol selectivity factor that is eight times smaller. These results reveal that the cross-linked MIP can distinguish the slightly different side chains of steroidal compounds. Moreover, cross-linking dramatically improves the sensitivity and selectivity of the MIP, increasing the rigidity of the binding cavity. In addition, the orientational assembly of the recognition cavities greatly affects their selectivity, as demonstrated by the significant non-specific binding of progesterone in the R-MIP.

In order to assess whether the proposed protocol can be applied to cortisol detection in real samples, a competitive fluorescent binding assay was conducted using the cross-linked MIP in a 10 vol% saliva solution. The  $\Delta I/I_0$  value clearly increases (electronic supplementary material, figure S12) with the cortisol concentration ( $K_a = 4.47 \times 10^{10} \text{ M}^{-1}$ ), and saturation is observed at approximately 0.6 nM, where the detectability is comparable to that of commercially available ELISA [63] and radioimmunoassay [64]. Although the  $\Delta I/I_0$  value is smaller than that obtained in the buffer solution (electronic supplementary material, figure S12), the apparent sensitivity is high enough to detect the cortisol secreted in human saliva (greater than 2 nM) [63]. The results clearly indicate that the MIP thin layer with oriented homogeneous cavities that contain dual binding sites developed herein exhibits effective cortisol recognition, and the highly sensitive detection of cortisol is confirmed by a competitive fluorescence assay using a real saliva sample.

### 3. Experimental set-up

#### 3.1. Preparation of the mixed self-assembled monolayer on the gold-coated glass substrate

A gold-coated glass substrate was washed with water and EtOH, dried with  $\text{N}_2$ , and then cleaned using a UV- $\text{O}_3$  cleaner (Bioforce Nanosciences) for 20 min. The substrate was then immersed in an EtOH solution (5 ml) containing bis[2-(2-bromoisobutyryloxy)undecyl]disulfide (1.5  $\mu\text{l}$ , 2.5  $\mu\text{mol}$ ) and 11-amino-1-undecanethiol hydrochloride (600  $\mu\text{g}$ , 2.5  $\mu\text{mol}$ ) at 25°C for 24 h.

#### 3.2. Immobilization of 6-NH<sub>2</sub>- $\beta$ -CD on the mixed self-assembled monolayer-modified substrate

The mixed SAM-modified substrate was immersed in a dimethylformamide (DMF) solution (5 ml) containing bis-dPEG<sub>4</sub>-NHS ester (12.2 mg, 25  $\mu\text{mol}$ ) at 25°C for 1 h. The resulting dPEG<sub>4</sub>-NHS-grafted substrate was then immersed in a DMF solution (5 ml) containing 6-NH<sub>2</sub>- $\beta$ -CD (17.0 mg, 15  $\mu\text{mol}$ ) at 25°C for 3 h.

#### 3.3. Preparation of molecularly imprinted polymers via SI-AGET ATRP

TM1 (3.50 mg, 5  $\mu\text{mol}$ ) was dissolved in dimethylsulfoxide (200  $\mu\text{l}$ ), and pure water (5 ml) was added. The  $\beta$ -CD-immobilized substrate was immersed in the above solution (5 ml), and incubated for 24 h at 25°C, and then washed with pure water and dried with  $\text{N}_2$ . A pre-polymerization solution (5 ml) containing  $\text{CuBr}_2$  (1.34 mg, 6  $\mu\text{mol}$ ), PMDETA (1.25  $\mu\text{l}$ , 6  $\mu\text{mol}$ ) and MPC (88.6 mg, 300  $\mu\text{mol}$ ) was added into a Schlenk flask, and a TM1-conjugated  $\beta$ -CD-immobilized substrate was inserted. To prepare the cross-linked MIP, MBAAm (9.25 mg, 60  $\mu\text{mol}$ ) was added to the above pre-polymerization solution. Degassing and nitrogen substitution were repeated, and then ascorbic acid (0.52 mg, 3  $\mu\text{mol}$ ) dissolved in degassed water (1.0 ml) was injected. SI-AGET ATRP was conducted for 30 min at 25°C. After polymerization, the

substrate was washed with pure water and immersed in a 1 M EDTA-4Na aqueous solution for 12 h at 25°C to remove Cu(II) ions. The substrate was then immersed into a 100 mM HCl aqueous solution for 12 h at 40°C to remove the cortisol-21-adamantane carboxylate moiety by hydrolysing the oxime bond. The substrate was washed with pure water and EtOH, and dried with N<sub>2</sub>.

### 3.4. Fluorescence-based competitive binding assay for cortisol using molecularly imprinted polymers and reference polymers

FITC-BPA (100 nM) dissolved in a 10 mM phosphate buffer (pH 7.4) was transferred into vials (5 ml), into which the polymer-coated substrates (MIPs and NIP) were inserted. The vials were incubated for 1 h at 25°C. Cortisol dissolved in a 10 mM phosphate buffer (pH 7.4) (final concentrations: 0 nM–0.4 nM for MIP, cross-linked MIP, RP-oxime, and R-MIP; 0–2 nM for RP-β-CD and NIP) was added. After 20 min at 25°C, the fluorescence intensities of the supernatants derived from free FITC-BPA that had been replaced by cortisol were measured (excitation wavelength: 495 nm, emission wavelength: 515 nm). For the selectivity experiments, structural analogues 17β-estradiol, cholesterol, testosterone and progesterone (0.2 nM for MIP, cross-linked MIP, RP-oxime and R-MIP; 1.5 nM for RP-β-CD and NIP) were employed as reference compounds.

### 3.5. Recovery tests for cortisol from diluted saliva samples

Saliva samples were collected by Saliva Collection Aid (Salimetrics, Inc., USA) and diluted to 11% (v/v) with a 10 mM phosphate buffer (pH 7.4). FITC-BPA was then added to the saliva samples (100 nM). The cross-linked MIP-coated substrate was immersed in the sample solutions and incubated for 1 h. Cortisol dissolved in the phosphate buffer (50 μl) was added (final concentrations: 0–1.1 nM, total volume: 1 ml), and incubated for 20 min at 25°C. Finally, fluorescence was measured in the supernatants (excitation wavelength: 495 nm, emission wavelength: 515 nm).

## 4. Conclusion

In this study, a novel template molecule (TM1) was designed for the preparation of MIP thin layers that are highly selective towards cortisol and possess oriented homogeneous cavities with dual binding sites. TM1 was copolymerized with MPC in the absence and presence of the cross-linker MBAAm via SI-AGET ATRP on a β-CD-immobilized gold-coated glass substrate. Highly sensitive detection of cortisol using the MIP thin layers was successfully demonstrated by a simple fluorescence-based competitive binding assay: the apparent limits of detection were 7.1 pM (without cross-linking:  $K_a = 1.28 \times 10^{11} \text{ M}^{-1}$ ) and 4.8 pM (with cross-linking:  $K_a = 2.30 \times 10^{11} \text{ M}^{-1}$ ) in aqueous solution, suggesting that the rigidity of the imprinted cavities induced a more precise recognition towards cortisol. The binding experiments using reference matrices, namely, NIP, RP-β-CD, RP-oxime and R-MIP, showed that the dual interaction in the imprinted cavity, that is, the hydrophobic interaction with β-CD and oxime formation with the aminoxy residues in the MIP thin layer, provided significantly high affinity and selectivity for cortisol. Sensitive cortisol detection was also demonstrated in real saliva samples. We believe that the proposed MIP preparation strategy can facilitate the application of MIPs not only for the diagnosis of mental disorders but also for other bio/chemical sensing tasks in the field of life sciences. This approach can pave the way for the development of artificial receptors capable of molecular recognition comparable with that of natural antibodies.

**Ethics.** All experiments using real saliva samples were approved by the Research Ethics Committee of the Graduate School of Engineering, Kobe University, Japan.

**Data accessibility.** All the relevant data is presented in this paper and in the electronic supplementary information.

**Authors' contributions.** T.T. conceived the study and supervised the experiments. N.S. designed and conducted the experiments. Y.Ka. measured the polymer film thickness and analysed the data. H.S. and Y.Ki. helped to design the experiments and analysed the data. All authors gave final approval for publication.

**Competing interests.** We declare we have no competing interests.

**Funding.** This work was partially supported by JSPS KAKENHI grant nos. 24651261 and 15K14943, and the Matching Planner Program from Japan Science and Technology Agency, JST (MP27115663368 and MP27115663207).

**Acknowledgement.** We thank Dr Tooru Ooya (Kobe University) for his kind suggestion.



## References

- Ginel PJ, Perez-Rico A, Moreno P, Lucena R. 1998 Validation of a commercially available enzyme-linked immunosorbent assay (ELISA) for the determination of cortisol in canine plasma samples. *Vet. Res. Commun.* **22**, 179–185. (doi:10.1023/A:1006021221409)
- Mostl E, Maggs JL, Schrotter G, Besenfelder U, Palme R. 2002 Measurement of cortisol metabolites in faeces of ruminants. *Vet. Res. Commun.* **26**, 127–139. (doi:10.1023/A:1014095618125)
- Carrozza C, Lapolla R, Gervasoni J, Rota CA, Locantore P, Pontecorvi A, Zuppi C, Persichilli S. 2012 Assessment of salivary free cortisol levels by liquid chromatography with tandem mass spectrometry (LC-MS/MS) in patients treated with mitotane. *Hormones* **11**, 344–349. (doi:10.14310/horm.2002.1363)
- Saiyudthong S, Suwannarat P, Trongwongsa T, Srisurapanon S. 2010 Comparison between ECL and ELISA for the detection of salivary cortisol and determination of the relationship between cortisol in saliva and serum measured by ECL. *Science Asia* **36**, 169–171. (doi:10.2306/scienceasia1513-1874.2010.36.169)
- Sellergren B. 2000 *Molecularly imprinted polymers*. Amsterdam, The Netherlands: Elsevier.
- Komiyama M, Takeuchi T, Mukawa T, Asanuma H. 2003 *Molecularly imprinting: from fundamentals to applications*. Weinheim, Germany: Wiley-VCH.
- Haupt K. 2012 *Molecular imprinting*. Berlin, Germany: Springer.
- Lee S-W, Kunitake T. 2013 *Handbook of molecular imprinting: advanced sensor applications*. Singapore: Pan Stanford Publishing.
- Wulff G. 1995 Molecular imprinting in cross-linked materials with the aid of molecular templates—a way towards artificial antibodies. *Angew. Chem. Int. Ed. Engl.* **34**, 1812–1832. (doi:10.1002/anie.199518121)
- Li S, Cao S, Whitcombe MJ, Piletsky SA. 2014 Size matters: challenges in imprinting macromolecules. *Prog. Polym. Sci.* **39**, 145–163. (doi:10.1016/j.progpolymsci.2013.10.002)
- Weisman A, Chou B, O'Brien J, Shea KJ. 2015 Polymer antidotes for toxin sequestration. *Adv. Drug Deliver. Rev.* **90**, 81–100. (doi:10.1016/j.addr.2015.05.011)
- Takeuchi T, Hayashi T, Ichikawa S, Kaji A, Masui M, Matsumoto H, Sasao R. 2016 Molecularly imprinted tailor-made functional polymer receptors for highly sensitive and selective separation and detection of target molecules. *Chromatography* **37**, 43–64. (doi:10.15583/jpchrom.2016.007)
- Ramström O, Ye L, Mosbach K. 1996 Artificial antibodies to corticosteroids prepared by molecular imprinting. *Chem. Biol.* **3**, 471–477. (doi:10.1016/S1074-5521(96)90095-2)
- Baggiani C, Baravalle P, Giovannoli C, Anfossi L, Giraudi G. 2010 Molecularly imprinted polymers for corticosteroids: analysis of binding selectivity. *Biosens. Bioelectron.* **26**, 590–595. (doi:10.1016/j.bios.2010.07.023)
- Matsui J, Higashi M, Takeuchi T. 2000 Molecularly imprinted polymer as 9-ethyladenine receptor having a porphyrin-based recognition center. *J. Am. Chem. Soc.* **122**, 5218–5219. (doi:10.1021/ja000064)
- Chen Y, Li X, Yin D, Li D, Bie Z, Liu Z. 2015 Dual-template docking oriented molecular imprinting: a facile strategy for highly efficient imprinting within mesoporous materials. *Chem. Commun.* **51**, 10 929–10 932. (doi:10.1039/C5CC03207E)
- Takeuchi T, Murase N, Maki H, Mukawa T, Shinmori H. 2006 Dopamine selective molecularly imprinted polymers via post-imprinting modification. *Org. Biomol. Chem.* **4**, 565–568. (doi:10.1039/B514432A)
- Takeda K, Kuwahara A, Ohmori K, Takeuchi T. 2009 Molecularly imprinted tunable binding sites based on conjugated prosthetic groups and ion-paired cofactors. *J. Am. Chem. Soc.* **131**, 8833–8838. (doi:10.1021/ja9004317)
- Yane T, Shinmori H, Takeuchi T. 2006 Atrazine transforming polymer prepared by molecular imprinting with post-imprinting process. *Org. Biomol. Chem.* **4**, 4469–4473. (doi:10.1039/B612407K)
- Lubke C, Lubke M, Whitcombe MJ, Vulfson EN. 2000 Imprinted polymers prepared with stoichiometric template—monomer complexes: efficient binding of ampicillin from aqueous solutions. *Macromolecules* **33**, 5098–5105. (doi:10.1021/ma00467u)
- Takeuchi T, Mori T, Kuwahara A, Ohta T, Oshita A, Sunayama H, Kitayama Y, Ooya T. 2014 Conjugated-protein mimics with molecularly imprinted reconstructible and transformable regions that are assembled using space-filling prosthetic groups. *Angew. Chem. Int. Ed.* **53**, 12 765–12 770. (doi:10.1002/anie.201406852)
- Miyata T, Jige M, Nakaminami T, Urugami T. 2006 Tumor marker-responsive behavior of gels prepared by biomolecular imprinting. *Proc. Natl Acad. Sci. USA* **103**, 1190–1193. (doi:10.1073/pnas.0506786103)
- Suga Y, Sunayama H, Ooya T, Takeuchi T. 2013 Molecularly imprinted polymers prepared using protein-conjugated cleavable monomers followed by site-specific post-imprinting introduction of fluorescent reporter molecules. *Chem. Commun.* **49**, 8450–8452. (doi:10.1039/C3CC40484F)
- Bai W, Gariano NA, Spivak DA. 2013 Macromolecular amplification of binding response in superaptamer hydrogels. *J. Am. Chem. Soc.* **135**, 6977–6984. (doi:10.1021/ja400576p)
- Horikawa R, Sunayama H, Kitayama Y, Takano E, Takeuchi T. 2016 A programmable signaling molecular recognition nanocavity prepared by molecular imprinting and post-imprinting modifications. *Angew. Chem. Int. Ed.* **55**, 13 023–13 027. (doi:10.1002/anie.201605992)
- Kugimiya A, Yoneyama H, Takeuchi T. 2000 Sialic acid imprinted polymer-coated quartz crystal microbalance. *Electroanalysis* **12**, 1322–1326. (doi:10.1002/1521-4109(200011)12:16<1322::AID-ELAN1322>3.0.CO;2-J)
- Shinde S, El-Schich Z, Malakpour A, Wan W, Dizayi N, Mohammadi R, Rurack K, Wingren AG, Sellergren B. 2015 Sialic acid-imprinted fluorescent core-shell particles for selective labeling of cell surface glycans. *J. Am. Chem. Soc.* **137**, 13 908–13 912. (doi:10.1021/jacs.5b08482)
- Bi X, Liu Z. 2014 Enzyme activity assay of glycoprotein enzymes based on a boronate affinity molecularly imprinted 96-well microplate. *Anal. Chem.* **86**, 959–966. (doi:10.1021/ac503778w)
- Bie Z, Chen Y, Ye J, Wang S, Liu Z. 2015 Boronate-affinity glycan-oriented surface imprinting: a new strategy to mimic lectins for the recognition of an intact glycoprotein and its characteristic fragments. *Angew. Chem. Int. Ed.* **54**, 10 211–10 215. (doi:10.1002/anie.201503066)
- Ma X, Liu J, Wu D, Wang L, Zhang Z, Xiang S. 2016 Ultrasensitive sensing of tris(2,3-dibromopropyl) isocyanurate based on the synergistic effect of amino and hydroxyl groups of a molecularly imprinted poly(o-aminophenol) film. *New J. Chem.* **40**, 1649–1654. (doi:10.1039/C5NJ02031J)
- Ma X, Wu D, Huang L, Wu Z, Xiang S, Chen S. 2015 Sensing 2,4,6-tribromophenol based on molecularly imprinted technology. *Monatsh. Chem.* **146**, 485–491. (doi:10.1007/s00706-014-1360-0)
- Ma X, Zhang Z, Zhang Y, Chen Z, Xiang S. 2014 Water-compatible imprinted polymers based on CS@SiO<sub>2</sub> particles for selective recognition of naringin. *J. Appl. Polym. Sci.* **131**, 40491. (doi:10.1002/APP40491)
- Ma X, Liu J, Zhang Z, Wang L, Xiang S. 2013 The cooperative utilization of imprinting, electro-spinning and a pore-forming agent to synthesise  $\beta$ -cyclodextrin polymers with enhanced recognition of naringin. *RSC Adv.* **3**, 25 396–25 402. (doi:10.1039/C3RA43062F)
- Murase N, Taniguchi S, Takano E, Kitayama Y, Takeuchi T. 2015 Fluorescence reporting of binding interactions of target molecules with core-shell-type cortisol-imprinted polymer particles using environmentally responsible fluorescent-labeled cortisol. *Macromol. Chem. Phys.* **216**, 1396–1404. (doi:10.1002/macp.201500665)
- Murase N, Taniguchi S, Takano E, Kitayama Y, Takeuchi T. 2016 A molecularly imprinted nanocavity-based fluorescence polarization assay platform for cortisol sensing. *J. Mater. Chem. B* **4**, 1770–1777. (doi:10.1039/C5TB02069G)
- Kamon Y, Matsuura R, Kitayama Y, Ooya T, Takeuchi T. 2014 Precisely controlled molecular imprinting of glutathione-s-transferase by orientated template immobilization using specific interaction with an anchored ligand on a gold substrate. *Polym. Chem.* **5**, 4764–4771. (doi:10.1039/C4PY00350K)
- Zhou XC, Zhou JH. 2006 Oligosaccharide microarrays fabricated on aminoxyacetyl functionalized glass surface for characterization of carbohydrate-protein interaction. *Biosens. Bioelectron.* **21**, 1451–1458. (doi:10.1016/j.bios.2005.06.008)
- Mazik M, Buthe AC. 2007 Oxime-based receptors for mono- and disaccharides. *J. Org. Chem.* **72**, 8319–8326. (doi:10.1021/jo701370g)
- Thygesen MB, Sauer J, Jensen KJ. 2009 Chemosensitive capture of glycans for analysis on gold nanoparticles: carbohydrate oxime tautomers provide functional recognition by proteins. *Chem. Eur. J.* **15**, 1649–1660. (doi:10.1002/chem.200801521)
- Villain M, Vizzavona J, Rose K. 2001 Covalent capture: a new tool for the purification of synthetic

- and recombinant polypeptides. *Cell Chem. Biol.* **8**, 673–679. (doi:10.1016/S1074-5521(01)00044-8)
41. Hishiyama T, Shibata M, Kakazu M, Asanuma H, Komiyama M. 1999 Molecularly imprinted cyclodextrins as selective receptors for steroids. *Macromolecules* **32**, 2265–2269. (doi:10.1021/ma9816012)
  42. Granadero D, Bordello J, Perez-Alvite MJ, Novo M, AlSoufi W. 2010 Host-guest complexation studied by fluorescence correlation spectroscopy: adamantane–cyclodextrin inclusion. *Int. J. Mol. Sci.* **11**, 173–188. (doi:10.3390/ijms11010173)
  43. Kwak ES, Gomez FA. 1996 Determination of the binding of  $\beta$ -cyclodextrin derivatives to adamantane carboxylic acids using capillary electrophoresis. *Chromatographia* **43**, 659–662. (doi:10.1007/BF02292984)
  44. Wang JS, Matyjaszewski K. 1995 Controlled/living radical polymerization. Halogen atom transfer radical polymerization promoted by a Cu(I)/Cu(II) redox process. *Macromolecules* **28**, 7901–7910. (doi:10.1021/ma00127a042)
  45. Wakioka M, Baek KY, Ando T, Kamigaito M, Sawamoto M. 2002 Possibility of living radical polymerization of vinyl acetate catalyzed by iron(I) complex. *Macromolecules* **35**, 330–333. (doi:10.1021/ma0115444)
  46. Cunningham MF. 2008 Controlled/living radical polymerization in aqueous dispersed systems. *Prog. Polym. Sci.* **33**, 365–398. (doi:10.1016/j.progpolymsci.2007.11.002)
  47. Haddleton DM, Crossman MC, Dana BH, Duncalf DJ, Heming AM, Kukulj D, Shooter AJ. 1999 Atom transfer radical polymerization of methyl methacrylate mediated by alkylpyridylmethanimine type ligands, copper(I) bromide, and alkyl halides in hydrocarbon solution. *Macromolecules* **32**, 2110–2119. (doi:10.1021/ma981670g)
  48. Zetterlund PB, Kagawa Y, Okubo M. 2009 Compartmentalization in atom transfer radical polymerization of styrene in dispersed systems: effects of target molecular weight and halide end group. *Macromolecules* **42**, 2488–2496. (doi:10.1021/ma900035x)
  49. Tanaka T, Okayama M, Kitayama Y, Kagawa Y, Okubo M. 2010 Preparation of 'mushroom-like' janus particles by site-selective surface-initiated atom transfer radical polymerization in aqueous dispersed systems. *Langmuir* **26**, 7843–7847. (doi:10.1021/la904701r)
  50. Kitayama Y, Takeuchi T. 2014 Localized surface plasmon resonance nanosensing of c-reactive protein with poly(2-methacryloyloxyethyl phosphorylcholine)-grafted gold nanoparticles prepared by surface-initiated atom transfer radical polymerization. *Anal. Chem.* **86**, 5587–5594. (doi:10.1021/ac501322x)
  51. Sasaki S, Ooya T, Kitayama Y, Takeuchi T. 2015 Molecularly imprinted protein recognition thin films constructed by controlled/living radical polymerization. *J. Biosci. Bioeng.* **119**, 200–205. (doi:10.1016/j.jbiosc.2014.06.019)
  52. Zhang YH, Tong AJ, Li LD. 2004 Synthesis of molecularly imprinted polymer with 7-chloroethyl-theophylline-immobilized silica gel as template and its molecular recognition function. *Spectrochim. Acta Mol. Biomol. Spectrosc.* **60**, 241–244. (doi:10.1016/S1386-1425(03)00225-7)
  53. Fu GQ, He HY, Chai ZH, Chen HC, Kong JA, Wang Y, Jiang YZ. 2011 Enhanced lysozyme imprinting over nanoparticles functionalized with carboxyl groups for noncovalent template sorption. *Anal. Chem.* **83**, 1431–1436. (doi:10.1021/ac1029924)
  54. Lin Z. A, Xia ZW, Zheng JN, Zheng D, Zhang L, Yang HH, Chen GN. 2012 Synthesis of uniformly sized molecularly imprinted polymer-coated silica nanoparticles for selective recognition and enrichment of lysozyme. *J. Mater. Chem.* **22**, 17 914–17 922. (doi:10.1039/c2jm32734a)
  55. Tan CJ, Chua MG, Ker KH, Tong YW. 2008 Preparation of bovine serum albumin surface-imprinted submicrometer particles with magnetic susceptibility through core–shell miniemulsion polymerization. *Anal. Chem.* **80**, 683–692. (doi:10.1021/ac701824u)
  56. Ishihara K, Ueda T, Nakabayashi N. 1990 Preparation of phospholipid polyliners and their properties as polymer hydrogel membranes. *Polym. J.* **22**, 355–360. (doi:10.1295/polymj.22.355)
  57. Kalia J, Raines RT. 2008 Hydrolytic stability of hydrazones and oximes. *Angew. Chem. Int. Ed.* **47**, 7523–7526. (doi:10.1002/anie.200802651)
  58. Zhang XW *et al.* 2011 Bisphenol A disrupts steroidogenesis in human H295R cells. *Toxicol. Sci.* **121**, 320–327. (doi:10.1093/toxsci/kfr061)
  59. Prasantha GK, Divya LM, Sadasivan C. 2010 Bisphenol-A can bind to human glucocorticoid receptor as an agonist: an *in silico* study. *J. Appl. Toxicol.* **30**, 769–774. (doi:10.1002/jat.1570)
  60. Tlili C, Myung NV, Shetty V, Mulchandani A. 2011 Label-free, chemiresistor immunosensor for stress biomarker cortisol in saliva. *Biosens. Bioelectron.* **26**, 4382–4386. (doi:10.1016/j.bios.2011.04.045)
  61. Frascioni M, Mazarino M, Botre F, Mazzei F. 2009 Surface plasmon resonance immunosensor for cortisol and cortisone determination. *Anal. Bioanal. Chem.* **394**, 2151–2159. (doi:10.1007/s00216-009-2914-6)
  62. Sesay AM, Micheli L, Tervo P, Palleschi G, Virtanen V. 2013 Development of a competitive immunoassay for the determination of cortisol in human saliva. *Anal. Biochem.* **434**, 308–314. (doi:10.1016/j.ab.2012.12.008)
  63. Aardal E, Holm A-C. 1995 Cortisol in saliva: reference ranges and relation to cortisol in serum. *Eur. J. Clin. Chem. Clin. Biochem.* **33**, 927–932. (doi:10.1515/ccbm.1995.33.12.927)
  64. Jung C, Greco S, Nguyen HHT, Ho JT, Lewis JG, Torpy DJ, Inder WJ. 2014 Plasma, salivary and urinary cortisol levels following physiological and stress doses of hydrocortisone in normal volunteers. *BMC Endocr. Disord.* **14**, 91–100. (doi:10.1186/1472-6823-14-91)